Near-infrared fluorescence imaging improves the nodal yield in neck dissection in oral cavity cancer — A randomized study

Anders Christensen [a, b, *], Karina Juhl [b], Katalin Kiss [c], Giedrius Lelkaitis [c], Birgitte Wittenborg Charabi [a], Jann Mortensen [b], Andreas Kjær [b], Christian von Buchwald [a]

[a] Department of Otolaryngology, Head & Neck Surgery and Audiology, Rigshospitalet, University of Copenhagen, Blegdamsvej 9, DK-2100, Copenhagen East, Denmark
[b] Department of Clinical Physiology, Nuclear Medicine & PET and Cluster for Molecular Imaging, Rigshospitalet, University of Copenhagen, Blegdamsvej 9, DK-2100, Copenhagen East, Denmark
[c] Department of Pathology, Rigshospitalet, University of Copenhagen, Blegdamsvej 9, DK-2100, Copenhagen East, Denmark

ARTICLE INFO

ABSTRACT

Introduction: Lymph node yield (LNY) in neck dissection has been identified as a prognostic factor in oral cavity cancer. The purpose of this study was to investigate the impact of additional use of optical imaging on LNY in therapeutic ND in oral cancer.
Methods: Consecutive patients with oral squamous cell carcinoma with clinical neck metastasis planned for primary tumor resection were randomized to conventional neck dissection or near-infrared fluorescence (NIRF)-guided neck dissection, respectively. In the intervention group, patients were injected with ICG-Nanocoll prior to surgery. Intraoperatively, an optical hand-held camera system was used for lymph node identification. Also, NIRF imaging of the neck specimen was performed, and optical signals were pinned with needle markings to guide the pathological examination. The endpoint of the study was LNY per neck side in levels Ib-III.
Results: 31 patients were included with 18 neck sides in the control group and 18 neck sides in the intervention group for evaluation. During NIRF-guided ND, individual lymph nodes could be identified by a bright fluorescent signal and individual tumor-related drainage patterns could be observed in the neck. The LNY in the intervention group was significantly higher compared to the control group ($p = 0.032$) with a mean of 24 LN (range: 12—33 LN in levels Ib-III compared to 18 LN (range: 10—36 LN) in the control group, respectively.
Conclusions: NIRF-guided ND significantly improved the nodal yield compared to the control group. Intraoperative real-time optical imaging enabled direct visualization of tumor-related drainage patterns within the neck lymphatics.

Introduction

Neck dissection (ND) is an integrated standard surgical procedure in head and neck cancer both for diagnostic and therapeutic purposes. Technically a neck dissection may be defined as the surgical removal of potential or verified cervical nodal metastatic disease including surrounding fibro-fatty tissue within anatomically defined compartments of the neck between the superficial subplatysmal fascia and the deep cervical fascia. Since systematic management of regional lymphatics by neck dissection was first described by Criel in 1906, the procedure has developed from a radical approach in direction of a selective approach with reduced surgical invasiveness and morbidity by sparing non-lymphatic structures, without compromising oncological safety [1,2]. The division of the neck compartment into levels by anatomical landmarks, as described in the Robbins classification, serves the important purposes, both to define the extent of a neck dissection

* Corresponding author. Department of Otolaryngology, Head & Neck Surgery and Audiology, Rigshospitalet, University of Copenhagen, Blegdamsvej 9, DK-2100, Copenhagen East, Denmark.
E-mail addresses: anders.christensen.03@regionh.dk (A. Christensen), karina.juhl@sund.ku.dk (K. Juhl), katalin.kiss@regionh.dk (K. Kiss), giedrius.lelkaitis@regionh.dk (G. Lelkaitis), birgitte.wittenborg.charabi@regionh.dk (B.W. Charabi), jann.mortensen@regionh.dk (J. Mortensen), andreas.kjaer@regionh.dk (A. Kjær), christian.von.buchwald@regionh.dk (C. von Buchwald).

intraoperatively, and to ensure a standardized systematical reporting of findings in the resected neck specimens [3]. The knowledge of reported patterns of metastatic spread to the neck from different tumor subsites in the upper digestive tract has allowed defining which levels should be included in the neck dissection [4].

Lymph node yield (LNY), defined as the total number of detected lymph nodes (LN) in a dissection specimen, is an established prognostic factor in several solid malignancies like colorectal, breast, bladder and esophageal cancer [5—8]. Equally, lymph node ratio (LNR), defined as the number of metastasis divided by the nodal yield, has been reported to be an independent prognosticator for outcome, that may serve as a tool to stratify patients for adjuvant therapy [9,10]. In head and neck cancer, accumulating evidence supports the importance of both LNY and LNR as powerful independent prognostic factors for outcome. However, their role in the selection of patients for either radiation or chemo-radiation remains unreconciled [11—13]. Also, as a metric for surgical treatment quality, LNY has been suggested as a tool to reflect the completeness or thoroughness of a neck dissection [14]. Currently, no consensus has been established regarding minimal threshold values of LNY or LNR in neck dissection [15]. In the newly updated 8th Edition AJCC/UICC staging manual a recommended minimal LNY of 6 nodes in an elective ND, and 15 nodes in a therapeutic ND, is stated, which is a very conservative guideline compared to reported thresholds in the bulk of published literature [16]. Inherently LNY, apart from the surgical procedure itself, also depends on the postoperative histological work-up in the process of identifying the lymph nodes [17].

Optical-guided surgery is a rapidly developing technology based on intraoperative real-time imaging of injected or intrinsic fluorescent molecules to aid surgical procedures. Both non-targeted and targeted strategies have been investigated, and the number of preclinical data is growing rapidly. Especially in oncological surgery, the concept of intraoperative real-time targeted imaging of tumor and metastatic disease to guide surgical resection holds a great potential to impact future cancer treatment [18]. Several applications of optical imaging using non-targeted Idocyanine Green (ICG) have been explored clinically, including optical-guided sentinel node biopsy (SNB) for staging the regional nodal basin in malignant melanoma, breast and cervical cancer [19—21]. Our group and others have previously investigated a combined radio- and optical-guided SNB technique using a bimodal tracer complex with beneficial hydrodynamic properties by mixing radioactive technetium-labeled Nanocoll and ICG [22,23]. In the current study we expanded the concept of SNB to identify neck nodes directly connected to the drainage from the primary tumor, by using a monomodal ICG-colloid tracer complex and optical imaging both intraoperatively during the neck dissection procedure, and for ex vivo assessment of the resected neck specimen. To our best knowledge, the possible influence of additional optical imaging on LNY in head and neck cancer has not previously been reported.

The objective of this study was to examine the potential influence of optical imaging on LNY compared to standard white light surgery in neck dissection in a randomized prospective study design.

Materials and methods

The study was conducted as a single-institution randomized clinical trial at the Department of Otolaryngology − Head & neck Surgery at Rigshospitalet, Copenhagen University hospital, which is a tertiary high-volume head and neck cancer referral center covering Eastern Denmark with a population of approximately 2.8 million. Patients with primary oral squamous cell carcinoma (OSCC)

and neck metastasis present at time of diagnosis (cT1-T4, N+) scheduled for primary tumor resection and therapeutic ND was included in the study. Staging was based on the 7th edition of the TNM AJCC/UICC system. Exclusion criteria were cN0 status, prior surgery or radiotherapy to the neck, severe kidney failure, pregnancy, known allergy to ICG or Iodine and untreated hyperthyroidism. Patients with cN0 status were excluded, because this patient group routinely is managed by SNB for staging of the neck as a standard procedure in our center and not elective ND. All patients were preoperatively evaluated by clinical examination, neck ultrasound, MRI and CT if bone involvement was suspected. The decision to perform unilateral or bilateral ND was made preoperatively in both study arms based on tumor location and laterality of neck metastasis. The study was monitored by the GCP unit of Copenhagen and conducted in accordance with the Helsinki Declaration. The study was approved by the Regional Scientific Ethical Committee, The Danish Medicines Agency and the European Medicines Agency (EudraCT 2013-003578-28, www. Clinicaltrialsregister.eu). Informed written consent was obtained before enrolment in the study.

The design was a non-blinded two-arm randomized study. The needed study sample in the control arm and the intervention arm was estimated from a power calculation, based on an alfa-value of 5%, a power of 80%, an enrolment ratio of 1:1 and a minimal relevant detected difference in LNY of 2/patient between the two groups. The estimated sample size was 14 neck sides/group, and we decided to include 18 neck sides in each group. The primary endpoint was LNY in levels Ib-III. The randomization was performed prior to trial initiation using a free-software random number generator (www.random.org) and the generated randomization key was stored by an external partner to be consulted for inclusion and subsequent randomization of individual consecutive patients.

Preparation of imaging agent

An ICG stock solution was prepared by adding 5 ml of sterile water to a vial of 25 mg of dry compound ICG (Pulsion Medical, Germany). Nanocoll (GE Healthcare, UK) was prepared by adding 2 ml of isotone saline water to a vial containing 0.5 mg of human albumin colloid (GE Healthcare, UK). Then 0.2 ml of the ICG solution and 0.2 ml of the Nanocoll was carefully mixed in a syringe and left for 5 min of incubation. The final mixture with a volume of 0.4 ml, containing 1 mg of ICG (3.2 mM) was prepared in a 1 ml syringe with a 25G needle for injection. Based on electron microscopy imaging it has been estimated, that the molar ICG/nanocoll ratio in the unconjuncgated ICG-Nanocoll tracer complex, where Nanocoll is saturated with ICG, is 61:1 [24]. The molar ICG/nanocoll ratio of the ICG-Nanocoll tracer complex used in this study was 1.800:1. Therefore, in the injected tracer preparation, a substantial part of ICG was unbound ICG, to allow rapid drainage to the entire tumor-related neck lymphatics. Patients were injected the day before or the day of surgery after application of local spray anesthesia in four submucosal peritumoral deposits.

Imaging and perioperative procedures

The tumor ablation procedure was performed prior to the neck procedure. In the oral cavity reconstruction was managed locally with or without local flaps, no free flaps was used. Optical imaging was performed with a Fluobeam 800 camera system (Fluoptics, France), which is a clinically approved device with accompanying software operated from a laptop. Real-time imaging was presented for the surgical team on a monitor and the camera head was brought to the surgical field in sterile draping for hand-held

maneuvering by a surgeon. During optical imaging, the surgical parabolic lights were turned away from the surgical field to avoid imaging interference. The system works with laser excitation (768 nm) and an autofocus function to allow movement-independent focused video imaging. In all cases the same surgical approach in the ND was applied through a single curved horizontal neck incision, and as a minimum levels Ib-III was included in the ND. Determined by extend and location of nodal metastasis, and by preference of the individual surgeons, levels Ia, IV, Va or Vb was also included. Specimens were divided on the table into individual levels. Mono-polar bovie knife was not used.

In the intervention group, optical navigation was first applied before skin incision to access transcutaneous signals and then intermittently during the ND. Finally, a systematic search was conducted of each dissected level strictly defined by the anatomical boundaries for optical signals left behind. It was recorded, if additional optical imaging of the neck following the completed ND caused further dissection and resection of fibro-fatty tissue containing LN. Further, on the back table in the OR each resected neck level specimen was mounted on a cork plate and optical imaging with the optical camera fixed on an in-house made surgical arm was performed. All hot spots of fluorescence suspected to be LN were marked with needles before being submitted for histopathological processing.

In the pathology department, neck specimens from the control group was managed according to a standard procedure, that included macroscopic inspection and manual palpation of the formalin-fixed tissues to identify and dissect individual LN. In the intervention group tissues from all needle markings in the specimens were secured for microscopy, before standard inspection and palpation for lymph nodes was performed. All secured tissues from neck specimens in both study arms were cut in 2 mm thick slices, paraffin embedded, routinely proceeded and 4 μm thick slides were stained for Hematoxylin and Eosin. The histological evaluation was done by a trained head and neck pathologist. Tumor deposits were classified as macrometastasis (ma, $\geq$ 2 mm), micrometastasis (mi, < 2 mm and $\geq$0.2 mm) or isolated tumor cells (ICT, < 0.2 mm) [25].

Data analysis

Data analysis was performed using SAS Enterprise software Version 9.4 (SAS Institute A/S, USA). A value of $p < 0.05$ was considered statistically significant, and two-sided testing was applied in all calculations. The primary endpoint, difference in LNY, was analyzed as a continuous viable by a Student T-test. For comparison of clinicopathological data between groups, Fisher's exact test, Chi Square test, Student T-test or Wilcoxon test were used when appropriate. Descriptive statistics are presented as mean, median, range and percentages.

Results

A total of 31 patients were included, with 15 patients in the control arm and 16 patients in the NIRF arm. Three patients in the control group, and 2 patients in the NIRF had bilateral ND, respectively. Therefore, in each group 18 neck-sides were available for evaluation (Table 1). Comparison of demographics and clinico-pathological variables between the two groups is presented in Table 2. No statistically significant differences were detected between the two groups. The overall cohort had a male dominance and the majority of the tumors were located on the tongue or in the floor of the mouth.

Intraoperatively in the NIRF group, optical imaging during ND allowed to detect individual LN embedded in fibro-fatty tissue with a well-demarked and bright signal (Fig. 2). In some cases, also lymphatic channels connected to individual LN could be presented due to ICG imaging. Ex vivo, imaging of individual neck level specimens on the back table showed a preserved and intense

Table 1
Patient cohort overview.

Case No.	Group	Age	Sex	T-site	cTNM	pTNM	ND	ND Laterality	Met location by level	Met number
2	Control	50	F	Floor of mouth	T2N1M0	T2N2bM0	Ia-III	Unilateral	1b	5 ma
5	Control	65	M	Lateral tongue	T3N1M0	T3N2bM0	Ib-III	Unilateral	2a +3	5 ma + 1 mi
7	Control	56	M	Floor of mouth	T2N2bM0	T2N2cM0	Ia-III, V	Bilateral	1b + 1a contralateral	1 ma + 1 mi
9	Control	75	F	Lower gum	T4aN1MO	T4N0M0	Ib-III	Unilateral	1 b	1b
11	Control	39	F	Buccal mucosa	T2N2bM0	T2N2bM0	Ib-III	Unilateral	1b	1 ma
14	Control	66	M	Floor of mouth	T2N1M0	T2N1M0	Ia-IV	Bilateral	1b	1 ma
16	Control	66	M	Floor of mouth	T3N1M0	T3N2bM0	Ia-IV	Unilateral	1b + 2b	2 ma
18	Control	71	M	Lateral tongue	T2N1M0	T2N1M0	Ib-III	Unilateral	2a	1 ma
20	Control	78	M	Lateral tongue	T3N1MO	T2N1M0	Ia-III	Unilateral	2a	1 ma
21	Control	63	M	Lateral tongue	T3N2cM0	T2N2cM0	Ia-III	Bilateral	1b, 2a, 3 contralateral	5 ma
23	Control	52	M	Inferior tungue	T3N2bM0	T2N2bM0	Ia-IV	Unilateral	1b, 2a	2 ma
26	Control	57	F	Floor of mouth	T4aN2bM0	T4aN2bM0	Ia-IV	Unilateral	3	2ma
28	Control	66	M	Lateral tongue	T2N1M0	T2N2bM0	Ia-III	Unilateral	2a	2 ma
29	Control	61	F	Retromolar region	T1N1M0	T2N1M0	Ib-III	Unilateral	2a	1 ma
32	Control	79	F	Buccal mucosa	T1N1M0	T1N1M0	Ia-IV	Unilateral	1b	1 ma
1	NIRF	55	M	Lateral tongue	T2N1M0	T2N2bM0	Ia-III	Unilateral	1a + 2a	2 ma
3	NIRF	55	M	Lateral tongue	T3N1M0	T3N1M0	Ia-III	Unilateral	2a	1 ma
6	NIRF	58	M	Floor of mouth	T3N1M0	T3N2bM0	Ia-III	Unilateral	1b	3 ma
8	NIRF	80	M	Buccal mucosa	T2N1M0	T2N2bM0	Ia-IV	Unilateral	1b + 2a	3 ma
10	NIRF	71	M	Lower gum	T1N1MO	T1N2bM0	Ia-III	Unilateral	1b + 3	2 ma
12	NIRF	42	M	Upper gum	T4aN1M0	T4aN1M0	Ia-IV	Unilateral	1b	1 ma
13	NIRF	68	M	Lateral tongue	T3N1M0	T4aN2bM0	Ib-III	Unilateral	1b + 2a	2 ma
15	NIRF	70	M	Floor of mouth	T2N1M0	T2N1M0	Ia-III	Bilateral	3	1 ma
17	NIRF	67	M	Lateral tongue	T1N1M0	T1N2bM0	Ia-III	Unilateral	1b	2 ma
19	NIRF	55	M	Lateral tongue	T2N2bM0	T2N2bM0	Ia-III	Unilateral	2a +3	12 ma
22	NIRF	63	M	Lower gum	T4aN1M0	T4N1M0	Ia-III	Unilateral	2a	1 ma
24	NIRF	67	M	Lateral tongue	T3N2cM0	T2N2cM0	Ia-IV	Unilateral	3, 2a	2 ma
25	NIRF	75	F	Lower gum	T2N2bM0	T2N2bM0	Ia-III	Unilateral	1b, 2a	3 ma
27	NIRF	82	F	Buccal mucosa	T1N1M0	T1N1M0	Ia-III	Unilateral	2a	1 mi
30	NIRF	56	M	Floor of mouth	T4aN2cM0	T4aN2cM0	Ia-III, V	Bilateral	1b + 1b and 3 contralateral	3 ma
31	NIRF	54	F	Retromolar region	T4aN1N0	T4N1M0	Ib-III	Unilateral	2a	1 ma

Table 2
Comparative statistics between study groups.

Variable	Control group N = 15	NIRF group N = 16	p value
Age[c] (mean)	63	64	0.64
Sex[a]			
Male	9	13	0.25
Female	6	3	
Tobacco[b]			
Pack years (mean)	36,9	34.2	0.65
Alcohol[a]			
Current	7	3	0.16
Former	1	4	
Never	7	9	
BMI[d] (mean)	21.9	24.8	0.21
T-site[a]			
Buccal	2	2	0.06
Upper gum	0	1	
Lower gum	1	3	
Hard palate	0	0	
Floor of mouth	5	4	
Lateral tongue	5	5	
Inferior tongue	1	0	
Retromolar region	1	1	
cTNM stage[b]			
Stage 3	9	11	0.61
Stage 4	6	5	
cT stage[a]			
T1	2	4	0.61
T2	7	5	
T3	5	3	
T4	2	4	
cN stage[a]			
N1	10	12	0.62
N2a	0	0	
N2b	4	2	
N2c	1	2	
pN stage[a]			
N1	7	6	0.88
N2a	0	0	
N2b	6	8	
N2c	2	2	
N-site up-staging[b]			
Yes	5	6	0.81
No	10	10	
N site procedure time[c] (mean)	116 min	90 min	0.06

[a] Fisher's exact test.
[b] Chi Square test.
[c] Student T-test.
[d] Wilcoxon rank sum test.

optical signal, which permitted readily placing of needle markings in individual hot spots (Fig. 3). In 13 out of 16 cases (81%), imaging of the completed neck levels led to additional resection of tissue guided by the optical signals detected. Eight of 16 patients (50%) had the tracer injection the day before surgery (mean 14 h, range 11–19 h) with no apparent difference in intraoperative imaging quality, compared to patients injected on the same day of surgery (data not shown). Pre-incision transcutaneous imaging of the neck detected localized signals in 3 of 16 cases (19%).

In one case, for exploratory purposes, the optical camera system was transferred to the department of pathology the day after surgery to perform imaging of a formalin fixed ND specimen. The individual optical signals marked with needles were found to be fully preserved after tissue fixation (data not shown).

A total of 390 LN were detected in the control group and 468 LN in the NIRF group after pathology workup of neck specimens. The mean LNY from ND level Ib-III was 18 LN (CI 95% 15.0–21.8, range: 10–36 LN) in the control group and 24 LN (CI 95% 20.8–27.2, range: 12–33 LN) in the NIRF group, respectively. The difference in LNY between the two groups was statistically significant (p = 0.016) (Fig. 1). In the NIRF group, 335 out of 468 resected LN (71.6%) were

identified ex vivo by the fluorescent signal and needle markings. In addition 24 out of 359 needle markings (6.7%) were false positive, as the optical signal did not represent LN on histology but only connective tissues. All LN metastasis confirmed on histology were in both groups located within level Ib-III and in the NIRF group all LN with metastasis were also identified by NIRF imaging. No adverse reactions related to the bimodal tracer agent occurred. No difference in metastatic yield, expressed as either pN stage or pathological N-site upstaging, between the two groups was observed (Table 2).

Discussion

This study showed a significantly improved LNY in therapeutic ND by additional use of an optical tracer compared to a control group with standardized comparison of the extent of dissected neck levels. By adapting the sentinel node concept, this technique enabled real-time intraoperative imaging of tumor-related lymphatic drainage to the neck basins. Not all LN in the neck were stained with tracer, as demonstrated with the needle markings, which indicates, that the neck lymphatics is not a completely interconnected meshwork of lymph nodes and lymphatic vessels. This observation correlates with findings from SNB studies in oral cavity cancer, where different drainage patterns in the neck from individual tumor subsites have been observed [26]. The tracer was designed to exhibit both retention in the first echelon nodes due to non-covalent binding of ICG to Nanocoll, and simultaneously to allow downstream drainage of excessive amount of non-bound ICG to the entire neck basin of each individual tumor. Hence, optical imaging of tumor-specific drainage may increase the chance of resecting potential subclinical metastatic lymph node deposits because of direct intraoperative guidance towards tumor-invaded nodes, which is the major course of failure in the neck following ND. The fundamental challenge in lymphadenectomy is not to resect as many nodes as possible, but to resect the right nodes that harbor clinically evident and subclinical metastatic disease to achieve N-site radicality. The limited number of optical false-positive findings was most likely due to transected lymphatic vessels and spillage of tracer agent into adjacent non-lymphatic tissues. Transcutaneous imaging of the lymphatic neck drainage was not feasible in this study. We have previously reported similar findings for ICG-based optical-guided SNB in the head and neck region [22]. The penetration depth of NIR photons in biological tissues is ½-1 cm, and the lymphatics below the platysma muscle seems to be located too deep to achieve adequate optical penetration for reliable imaging.

For comparison, only a limited number of papers concerning optical imaging of ND have been published. Digonnet and colleges demonstrated, in a series of 11 patients with HNSCC of different sub-sites, the ability of intravenously injected ICG to distinguish metastatic LN from negative nodes during ND based on a difference in signal intensity [27]. Similar, in preclinical models, Ashitate et al. investigated combined SNB and imaging of the entire nodal basin by local and systemic injection respectively of two fluorophores with different emission spectrums [28]. Both these studies used systemic administration of fluorescent dyes looking for differences in perfusion of lymphatics to image regional lymph node basins that differs from the current study, where passive drainage from the tumor site to the neck lymphatics was explored. To achieve tracer drainage to the entire neck lymphatics, and not only a subset of tumor-connected lymphatics, we propose several injection points in the oral cavity guided by known drainage patterns from different subsites deducted from SNB studies.

In contrast, optical-guided SNB using different tracer agents in head and neck cancer have been investigated in several studies. Use

| Group	N	Median	Mean	CI (95%)	Range
Control	18	16.5	18.3	15.1-22.2	10-36
NIRF	18	25.5	24.0	20.4-27.3	12-33
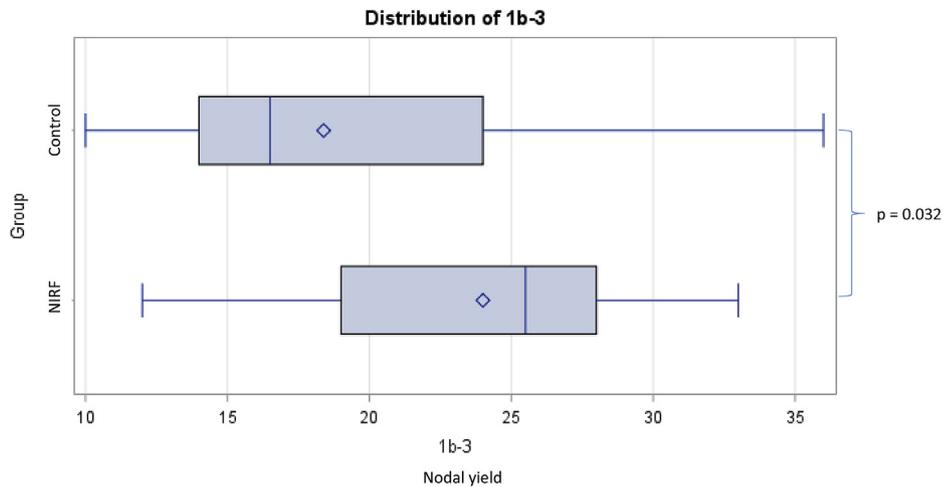
Fig. 1. LNY/neck side level 1b-3.
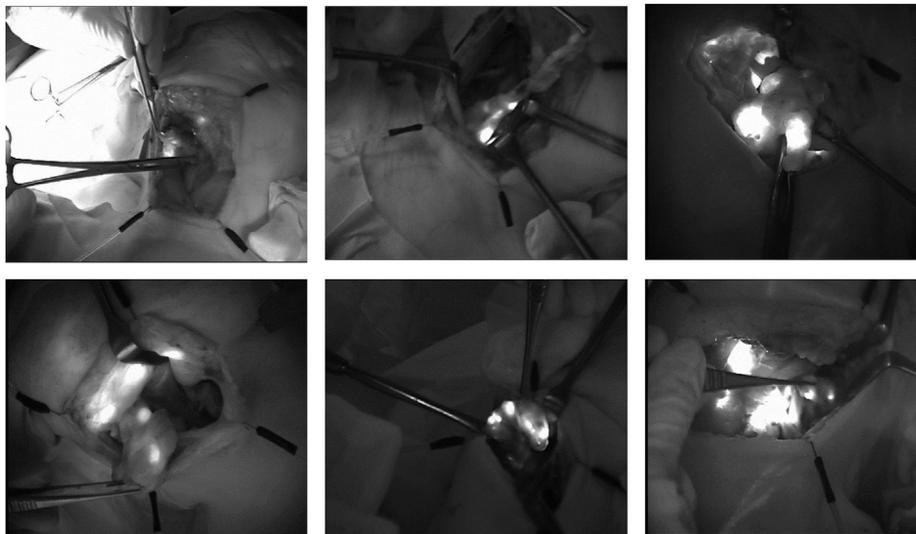
Fig. 2. NIRF imaging of neck lymphatics. Representative examples from six different patients of real-time intraoperative imaging of optical-guided ND with a Fluobeam camera system. Gray scale optical imaging merged on black and white video imaging was presented for the surgical team on a monitor. Individual LNs are seen with a bright optical signal sharply demarcated from the adjacent fibro-fatty tissue in the surgical field.

of unmixed ICG, either alone or together with a radiotracer administrated as separate injections has been studied in oral an oropharyngeal cancer [29–32]. Two of these studies reported suboptimal retention in the SN with inappropriate overflow of tracer to down-stream neck lymphatics [29,31]. These findings were most likely caused by the known fast transit time of ICG in the lymphatic system, and the moderate and transient retention of ICG in the SN. Traditionally Blue Dye has been used for SNB to visualize lymphatic drainage in OSCC and other malignancies, in a similar way to the use of ICG. However, several studies have shown, that methylene blue was outperformed by ICG for SNB due to superior retention in the SN [33–35].

Optimal retention in the SN can be achieved by mixing ICG with a colloid, to form a non-convantly bound tracer complex with favorable hydrodynamic properties. In addition, combined optical- and radio-guided SNB is feasible which has been demonstrated in OSCC and other malignancies in the head and neck region [22,23,36].

In this study we combined the retention effect of a colloid and the limited retention of unbound ICG to achive a tracer agent that exhibited retention in first echelon nodes, that most likely will contain clinical or subclinical metastasis, and simultaneous drainage of unbound ICG to down-stream neck lymphatics. We decided not to perform radioactive labeling of the tracer compound in this study because the aim was not SNB staging but therapeutic ND. Also, in OSCC the nodal template for SN distribution is well
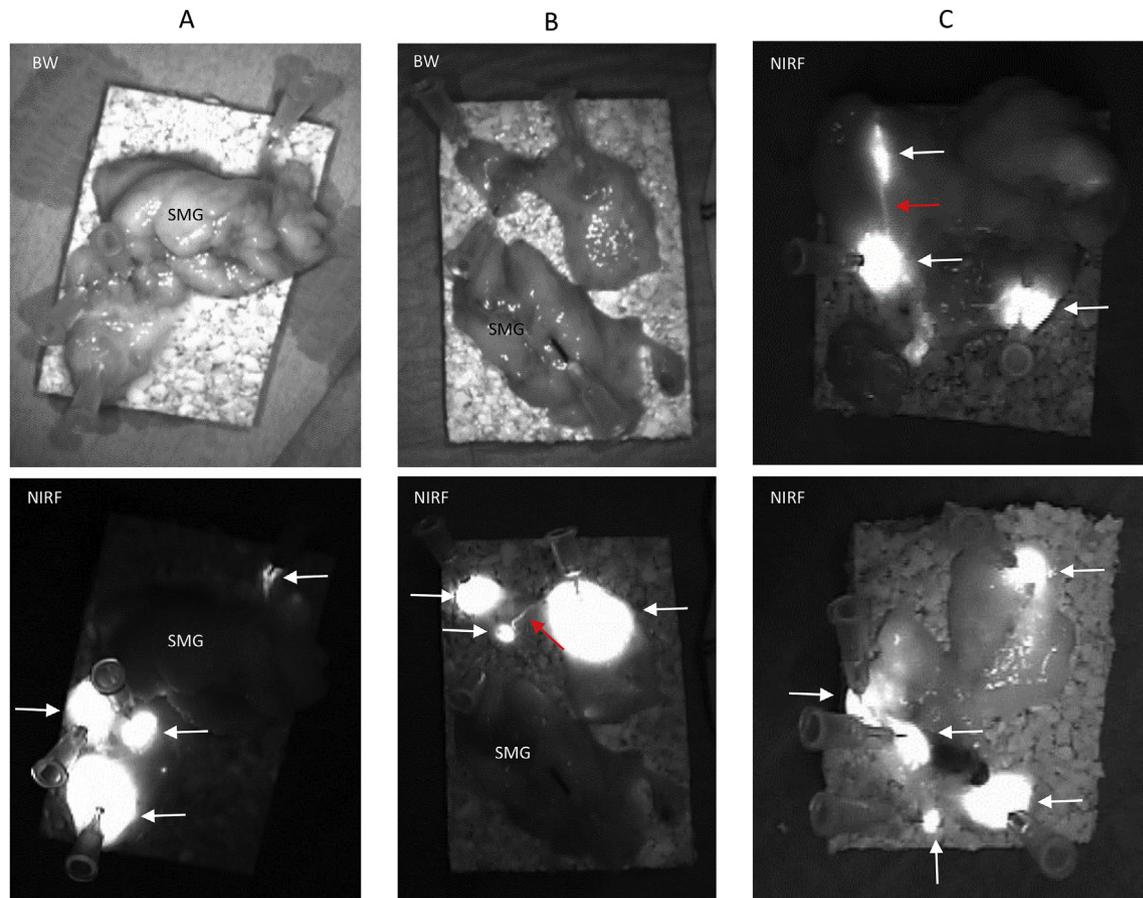
Fig. 3. Ex vivo NIRF imaging of ND specimens. A and B: Examples of imaging of level 1 specimens from two different cases. Black and white (BW) imaging upper row, NIRF imaging lower row. SMG = submandibular gland. C: Examples of NIRF imaging of level 3 specimens from two different cases. Needles were placed in individual NIRF signals (white single arrow). Optical imaging allowed identification of interconnecting lymphatic vessels (red arrow).

characterized and metastatic spread outside neck levels I-IV is rare. For comparison, in prostate cancer the metastatic distribution pattern is more unpredictable and bimodal ICG-Technetium99m-Nanocoll for SNB staging has proved valuable to detect SN outside the expected draining nodal basins [37]. Hence, radio-labeling would in theory have allowed to detect bilateral or contralateral lymphatic drainage preoperatively on SPECT/CT to aid surgical planning.

Many reports on LNY in ND differ in type of ND performed or lack information about the extent of ND by levels, hence direct comparison of yields and suggested cut-off values is difficult [11]. In addition, most previous reports were based on LNY in elective ND in cN0 cases. However, the mean LNY in therapeutic ND has been reported to be higher compared to elective ND. For example, in a retrospective study based on SEER data from 4618 OSCC patients, Kuo and colleges found a median LNY in cN0 and in cN + cases of 20 LN and 25 LN, respectively. Same study established statistically prognostic cut-off values for LNY of 16 LN in cN0 necks and 26 LN in cN + necks [38]. Interestingly, only the group, who had optical-guided ND in this study, had a comparable median LNY of 26 LN. As both LNY itself and LNR, that incorporates LNY, have been strongly associated with survival outcome in head and neck cancer, it is plausible that the proposed technique of optical imaging in the current study will have impact of patient outcome as well. Further high-powered clinical studies of optical-guided ND and a possible impact on survival outcome are warranted.

The positive effect of optical-assisted ND on LNY is most likely a combination of increased LN detection both intraoperatively as well as during histological processing. However, we did not specifically in this study investigate the individual effect of optical imaging on surgery and histological workup, respectively. In 81% of cases additional dissection was undertaken due to optical imaging, most often in level 1 below the edge of the mandible and in level 3 posterior to the internal jugular vein. In the initial assessment of the neck level specimens, needle markings identified small LN, which very likely would not have been detected by standard technique with inspection and palpation. As optical guidance in this study resulted in a higher LNY compared to a control group, most likely due to both the adequacy of the surgery, and the thorough-ness of the pathological workup, this technique may be of special importance for head and neck surgeons and pathologists during training of these procedures to improve learning curves and as a tool for quality metrics [39]. Because optical guidance caused additional dissection within the anatomically defined neck levels in the majority of the patients, there is a possible risk that this approach could increase the morbidity, in particular damage of the marginal branch of the facial nerve and the spinal accessory nerve. Morbidity from ND in the two study arms was not an endpoint in this study, but along with possible impact on survival outcome, change in morbidity should be investigated in clinical studies ahead.

The principle of optical-guided ND was feasible, and it did not prolong the neck procedure compared to the control group (Table 2). However, the need to intermittently turn away surgical

lights to perform optical imaging was inconvenient for the surgeons, and interference with lights from head lights was a challenge. In a future setup, a camera system with video color and merging of the optical signal unaffected by ambient light to optimize the intraoperative integration of optical imaging and surgical workflow is requested.

The sample size of the study was a limitation. Further, the results stem from a single-institution experience and individual technique among surgeons may have introduced elements of bias. Also, because a possible effect of a device applied intraoperatively was explored, blinding each surgeon to the type of ND in the two study arms was not technically possible. This study design may be a possible source for bias. The study did not include survival outcome and therefore did not investigate a possible impact of optical-guided ND on survival.

Conclusions

The results in this study revealed in a clinical setting a significantly higher LNY in OSCC patients with clinically node-positive necks achieved by optical-assisted ND compared to a control group in a randomized study design. Preoperative peritumoral injection of an ICG-based tracer formulation permitted real-time imaging of tumor-related drainage to the neck lymphatics to identify individual LN intraoperatively as well as postoperatively in dissected specimens. Further studies should be directed at investigating optical-guided lymphadenectomy in other types of malignancies with regional metastatic spread and the possible impact of survival outcome due increased LNY.

Disclosure

None.

Conflict of interest statement

GE Health care supported the study with Nanocoll free of charge. GE Health Care had no influence on the preparation of the protocol, conduction of the study, data interpretation or preparation of the manuscript.

References

[1] Crile G III . On the technique of operations upon the head and neck. Ann Surg 1906;44:842–50.
[2] Coskun HH, Medina JE, Robbins KT, Silver CE, Strojan P, Teymoortash A, et al. Current philosophy in the surgical management of neck metastases for head and neck squamous cell carcinoma. Head Neck 2015;37:915–26.
[3] Ferlito A, Robbins KT, Shah JP, Medina JE, Silver CE, Al-Tamimi S, et al. Proposal for a rational classification of neck dissections. Head Neck 2011;33:445–50.
[4] Lindberg R. Distribution of cervical lymph node metastases from squamous cell carcinoma of the upper respiratory and digestive tracts. Cancer 1972;29:
1446–9.
[5] Chen SL, Bilchik AJ. More extensive nodal dissection improves survival for stages I to III of colon cancer: a population-based study. Ann Surg 2006;244:602–10.
[6] Peyre CG, Hagen JA, DeMeester SR, Altorki NK, Ancona E, Griffin SM, et al. The number of lymph nodes removed predicts survival in esophageal cancer: an international study on the impact of extent of surgical resection. Ann Surg 2008;248:549–56.
[7] Wu SG, Wang Y, Zhou J, Sun JY, Li FY, Lin HX, et al. Number of negative lymph nodes should be considered for incorporation into staging for breast cancer. Am J Cancer Res 2015;5:844–53.
[8] Li F, Hong X, Hou L, Lin F, Chen P, Pang S, et al. A greater number of dissected lymph nodes is associated with more favorable outcomes in bladder cancer treated by radical cystectomy: a meta-analysis. Oncotarget 2016;7:61284–94.
[9] Hung M, Xu J, Nielson D, Bounsanga J, Gu Y, Hansen AR, et al. Evaluating the prediction of breast cancer survival using lymph node ratio. J Breast Cancer 2018;21:315–20.
[10] Moug SJ, Oliphant R, Balsitis M, Molloy RG, Morrison DS. The lymph node ratio optimises staging in patients with node positive colon cancer with implications for adjuvant chemotherapy. Int J Colorectal Dis 2014;29:599–604.
[11] Cheraghlou S, Otremba M, Kuo Yu P, Agogo GO, Hersey D, Judson BL. Prognostic value of lymph node yield and density in head and neck malignancies. Otolaryngol Head Neck Surg 2018;158:1016–23.
[12] Patel SG, Amit M, Yen TC, Liao CT, Chaturvedi P, Agarwal JP, et al. Lymph node density in oral cavity cancer: results of the International Consortium for Outcomes Research. Br J Canc 2013;109:2087–95.
[13] Ebrahimi A, Clark JR, Amit M, Yen TC, Liao CT, Kowalski LP, et al. Minimum nodal yield in oral squamous cell carcinoma: defining the standard of care in a multicenter international pooled validation study. Ann Surg Oncol 2014;21:3049–55.
[14] Divi V, Harris J, Harari PM, Cooper JS, McHugh J, Bell D, et al. Establishing quality indicators for neck dissection: correlating the number of lymph nodes with oncologic outcomes (NRG Oncology RTOG 9501 and RTOG 0234). Cancer 2016;122:3464–71.
[15] Norling R, Therkildsen MH, Bradley PJ, Nielsen MB, von Buchwald C. Nodal yield in selective neck dissection. Acta Otolaryngol 2013;133:965–71.
[16] Amin MB, Edge SB. American joint committee on cancer. AJCC cancer staging manual. Springer; 2017.
[17] Marres CC, de Ridder M, Hegger I, van Velthuysen ML, Hauptmann M, Navran A, et al. The influence of nodal yield in neck dissections on lymph node ratio in head and neck cancer. Oral Oncol 2014;50:59–64.
[18] Nguyen QT, Tsien RY. Fluorescence-guided surgery with live molecular navigation–a new cutting edge. Nat Rev Canc 2013;13:653–62.
[19] Knackstedt RW, Couto RA, Gastman B, et al. Indocyanine green fluorescence imaging with lymphoscintigraphy for sentinel node biopsy in head and neck melanoma. J Surg Res 2018;228:77–83.
[20] Sugie T, Kinoshita T, Masuda N, Sawada T, Yamauchi A, Kuroi K, et al. Evaluation of the clinical utility of the ICG fluorescence method compared with the radioisotope method for sentinel lymph node biopsy in breast cancer. Ann Surg Oncol 2016;23:44–50.
[21] Frumovitz M, Plante M, Lee PS, Sandadi S, Lilja JF, Escobar PF, et al. Near-infrared fluorescence for detection of sentinel lymph nodes in women with cervical and uterine cancers (FILM): a randomised, phase 3, multicentre, non-inferiority trial. Lancet Oncol 2018;19:1394–403.
[22] Christensen A, Juhl K, Charabi B, Mortensen J, Kiss K, Kjaer A, et al. Feasibility of real-time near-infrared fluorescence tracer imaging in sentinel node biopsy for oral cavity cancer patients. Ann Surg Oncol 2016;23:565–72.
[23] van den Berg NS, Brouwer OR, Klop WM, Karakullukcu B, Zuur CL, Tan IB, et al. Concomitant radio- and fluorescence-guided sentinel lymph node biopsy in squamous cell carcinoma of the oral cavity using ICG-(99m)Tc-nanocolloid. Eur J Nucl Med Mol Imaging 2012;39:1128–36.
[24] Buckle T, van Leeuwen AC, Chin PT, Janssen H, Muller SH, Jonkers J, et al. A self-assembled multimodal complex for combined pre- and intraoperative imaging of the sentinel lymph node. Nanotechnology 2010;21:355101.
[25] Hermanek P, Hutter RV, Sobin LH, Wittekind C. International Union against Cancer. Classification of isolated tumor cells and micrometastasis. Cancer 1999;86:2668–73.
[26] Schilling C, Stoeckli SJ, Haerle SK, Broglie MA, Huber GF, Sorensen JA, et al. Sentinel European Node Trial (SENT): 3-year results of sentinel node biopsy in oral cancer. Eur J Cancer 2015;51:2777–84.
[27] Digonnet A, van Kerckhove S, Moreau M, Willemse E, Quiriny M, Ahmed B, et al. Near infrared fluorescent imaging after intravenous injection of indocyanine green during neck dissection in patients with head and neck cancer: a feasibility study. Head Neck 2016;38(Suppl 1):E1833–7.
[28] Ashitate Y, Hyun H, Kim SH, Lee JH, Henary M, Frangioni JV, et al. Simultaneous mapping of pan and sentinel lymph nodes for real-time image-guided surgery. Theranostics 2014;4:693–700.
[29] Bredell MG. Sentinel lymph node mapping by indocyanin green fluorescence imaging in oropharyngeal cancer - preliminary experience. Head Neck Oncol 2010;2:31.
[30] Murase R, Tanaka H, Hamakawa T, Goda H, Tano T, Ishikawa A, et al. Double sentinel lymph node mapping with indocyanine green and 99m-technetium-tin colloid in oral squamous cell carcinoma. Int J Oral Maxillofac Surg 2015;44:1212–7.
[31] Nakamura T, Kogashiwa Y, Nagafuji H, Yamauchi K, Kohno N, et al. Validity of

sentinel lymph node biopsy by ICG fluorescence for early head and neck cancer. Anticancer Res 2015;35:1669–74.

[32] Peng H, Wang SJ, Niu X, Yang X, Chi C, Zhang G. Sentinel node biopsy using indocyanine green in oral/oropharyngeal cancer. World J Surg Oncol 2015;13: 278.

[33] Matheron HM, van den Berg NS, Brouwer OR, Kleinjan GH, van Driel WJ, Trum JW, et al. Multimodal surgical guidance towards the sentinel node in vulvar cancer. Gynecol Oncol 2013;131:720–5.

[34] van der Vorst JR, Schaafsma BE, Verbeek FP, Hutteman M, Mieog JS, Lowik CW, et al. Randomized comparison of near-infrared fluorescence imaging using indocyanine green and 99(m) technetium with or without patent blue for the sentinel lymph node procedure in breast cancer patients. Ann Surg Oncol 2012;19:4104–11.

[35] Fujisawa Y, Nakamura Y, Kawachi Y, Otsuka F. Indocyanine green fluorescence-navigated sentinel node biopsy showed higher sensitivity than the radioisotope or blue dye method, which may help to reduce false-negative cases in skin cancer. J Surg Oncol 2012;106:41–5.

[36] Frontado, Brouwer OR, van den Berg NS, Matheron HM, Vidal-Sicart S, van Leeuwen FW, et al. Added value of the hybrid tracer indocyanine green-99mTc-nanocolloid for sentinel node biopsy in a series of patients with different lymphatic drainage patterns. Rev Española Med Nucl Imagen Mol 2013;32:227–33.

[37] KleinJan GH, van Werkhoven E, van den Berg NS, Karakullukcu MB, Zijlmans H, van der Hage JA, et al. The best of both worlds: a hybrid approach for optimal pre- and intraoperative identification of sentinel lymph nodes. Eur J Nucl Med Mol Imaging 2018;45:1915–25.

[38] Kuo P, Mehra S, Sosa JA, Roman SA, Husain ZA, Burtness BA, et al. Proposing prognostic thresholds for lymph node yield in clinically lymph node-negative and lymph node-positive cancers of the oral cavity. Cancer 2016;122: 3624–31.

[39] Morton RP, Gray L, Tandon DA, Izzard M, McIvor NP. Efficacy of neck dissection: are surgical volumes important? The Laryngoscope 2009;119:1147–52.